ESKİŞEHİR TEKNİK ÜNİVERSİTESİ BİLİM VE TEKNOLOJİ DERGİSİ B- TEORİK BİLİMLER

Eskişehir Technical University Journal of Science and Technology B- Theoritical Sciences

2018, 6(2), pp. 193 - 205, DOI: 10.20290/aubtdb.396560

SOLITARY WAVE SIMULATIONS OF COMPLEX MODIFIED KORTEWEG-DE VRIES (CMKdV) EQUATION USING QUINTIC TRIGONOMETRIC B-SPLINE

Özlem ERSOY HEPSON *

Department of Mathematics-Computer, Faculty of Art & Science, Eskişehir Osmangazi University, Eskişehir, Turkey

ABSTRACT

The complex modified Korteweg-de Vries (CMKdV) equation is solved numerically using collocation method based on quintic trigonometric B-Splines. A Crank Nicolson rule is used to discretize in time. The well-known examples, propagation of bell-shaped initial pulse and collision of multi solitary waves are simulated using Matlab programme language. Computational results are examined by calculation of the accuracy of the method in terms of maximum error norm and the three conservation laws I_1, I_2 and I_3. Because the absolute changes of the lowest three laws are also good indicators of valid results even when the analytical solutions do not exist.

Keywords: Complex modified Korteweg-de Vries equation, Trigonometric B-Splines, Finite elements method, Solitary waves, Conservation laws

KOMPLEKS MODIFIYE KORTEWEG-DE VRIES (CMKdV) DENKLEMİNİN KUİNTİK TRİGONOMETRİK B-SPLİNE KULLANILARAK SOLİTARY DALGA SİMULASYONLARI

Matematik-Bilgisayar Bölümü, Fen-Edebiyat Fakültesi, Eskişehir Osmangazi Üniversitesi, Eskişehir, Türkiye

ÖZET

Bu çalışmada, kompleks modifiye Korteweg-de Vries (CMKdV) denklemi, kuintik trigonometrik B-spline tabanlı kolokasyon yöntemi ile nümerik olarak çözülmüştür. Zaman ayrışımı için Crank-Nicolson yöntemi kullanılmıştır. Oldukça iyi bilinen bazı test problemlerinin, Matlab programlama dili kullanılarak simulasyonu yapılmıştır. Korunum kanunlarındaki mutlak değişiklikler, analitik çözümler olmadığında bile geçerli sonuçların iyi göstergeleri olduğundan, yöntemin doğruluğu, maksimum hata normu ve I_1, I_2 and I_3 korunum kanunları cinsinden hesaplanarak, sonuçlar incelenmiştir.

Anahtar Kelimeler: Kompleks modifiye Korteweg-de Vries denklemi, Trigonometrik B-Spline, Sonlu elemanlar yöntemi, Solitary dalgalar, Korunum kanunları

1. INTRODUCTION

The complex modified Korteweg-de Vries (CMKdV) equation in the following form

$$\frac{\partial w}{\partial t}+\frac{\partial^3 w}{\partial x^3}+\alpha\frac{\partial(|w|w)}{\partial x}=0 \qquad (1)$$

where the subscripts x and t denote partial differentiation, α is a real parameter and $i=\sqrt{-1}$. $w(x,t)$ is a complex-valued function.

Some exact solutions to the CMKdV equation have been determined by various techniques like sine-cosine and tanh methods [1]. Since the CMKdV has an analytical solution, it has been used as a test problem to check the validity of the numerical methods by researchers. The numerical methods such as the split-step Fourier method (SSFM) [2], parallel split-step Fourier method [3], collocation method

*Corresponding Author: ozlemersoy88@gmail.com
Received: 28.12.2017 Accepted: 22.06.2018

[4-5], Galerkin method [6], differential quadrature method [7-8], finite difference method [12] are applied to obtain numerical simulations of this equation.

The B-splines are the known alternative basis functions providing continuity of some degree depending on the choice of the type of the B-splines. So far, many works have been done to show the efficiency of the B-spline functions of various orders covering finite elements, spectral and differential quadrature methods [9-11]. Especially the combination of B-splines is used as an approximation solution in collocation scheme to to solve the differential equations. Most researchers have choosen the collocation method for determination of the unknown parameters of the approximate solution in the finite elements method (FEM) formulation since writing FEM program based on the collocation together B-spline is easier than other techniques. The use of the trigonometric B-splines is not common for numerical methods to solve differential equations. The numerical approaches to solve a type of ODE with trigonometric B-splines for degree 2 and 3 are given by A. Nikolis [13-14]. Recently, trigonometric cubic B-spline collocation procedures are set up to solve the hyperbolic type problem, non classical diffusion problem and RLW, Fisher and Burgers' equation [15-19]. The few papers have come out dealing with solutions of the differential equations using quintic trigonometric B-spline. This study aims to fill the gap in the related literature by solving some initial boundary value problems constructed on CMKdV equation. For this purpose, the numerical solution of CMKdV equation by use of the collocation method based on the quintic trigonometric B-splines is given. To do this, boundary conditions

$$\begin{aligned} w(a,t) &= w(b,t) = 0, t \geq 0 \\ w'(a,t) &= w'(b,t) = 0, t \geq 0 \\ w''(a,t) &= w''(b,t) = 0, t \geq 0 \end{aligned} \tag{2}$$

and initial condition

$$w(x,0) = f(x), a \leq x \leq b \tag{3}$$

will be used according to test problem.

2. CONVERTING CMKdV TO A REAL PDE SYSTEM

We use the transformation

$$w(x,t) = u(x,t) + iv(x,t) \tag{4}$$

to decompose $w(x,t)$ into its real and imaginary parts, and get the real valued-modified Korteweg-de Vries (MKdV) equation system

$$\begin{aligned} \frac{\partial u}{\partial t} + \frac{\partial^3 u}{\partial x^3} + \alpha(3u^2 + v^2)\frac{\partial u}{\partial x} + 2\alpha uv\frac{\partial v}{\partial x} = 0 \\ \frac{\partial v}{\partial t} + \frac{\partial^3 v}{\partial x^3} + 2\alpha uv\frac{\partial u}{\partial x} + \alpha(3v^2 + u^2)\frac{\partial v}{\partial x} = 0 \end{aligned} \tag{5}$$

This system include the third-order derivatives with respect to space variable so that smooth approximation can be done with the quintic trigonometric B-splines.

3. NUMERICAL METHOD

Consider a uniform partition of the problem domain $[x_0 = a, x_N = b]$ with the points x_m, $m = 0,1,\dots,N$ and $h = (b-a)/N$ and the ghost points x_{-3}, x_{-2}, x_{-1}, x_{N+1}, x_{N+2}, x_{N+3} positioned outside the problem interval. Gost grid points are necessary to construct quintic B-splines basis on problem domain. Trigonometric quintic B-spline functions $T_m(x)$, $m = -2,\dots,N+2$ are defined at the nodes x_m by [20]

$$T_m(x)=\frac{1}{\theta}\begin{cases}\tau^5(x_{m-3}) & ,x_{m-3}\le x<x_{m-2}\\ -\tau^4(x_{m-3})\tau(x_{m-1})-\tau^3(x_{m-3})\tau(x_m)\tau(x_{m-2}) \\ -\tau^2(x_{m-3})\tau(x_{m+1})\tau^2(x_{m-2})-\tau(x_{m-3})\tau(x_{m+2})\tau^3(x_{m-2}) & ,x_{m-2}\le x<x_{m-1}\\ -\tau(x_{m+3})\tau^4(x_{m-2}) \\ \tau^3(x_{m-3})\tau^2(x_m)+\tau^2(x_{m-3})\tau(x_{m+1})\tau(x_{m-2})\tau(x_m) \\ +\tau^2(x_{m-3})\tau^2(x_{m+1})\tau(x_{m-1})+\tau(x_{m-3})\tau(x_{m+2})\tau^2(x_{m-2})\tau(x_m) \\ +\tau(x_{m-3})\tau(x_{m+2})\tau(x_{m-2})\tau(x_{m+1})\tau(x_{m-1}) \\ +\tau(x_{m-3})\tau^2(x_{m+2})\tau^2(x_{m-1})+\tau(x_{m+3})\tau^3(x_{m-2})\tau(x_m) & ,x_{m-1}\le x<x_m\\ +\tau(x_{m+3})\tau^2(x_{m-2})\tau(x_{m+1})\tau(x_{m-1}) \\ +\tau(x_{m+3})\tau(x_{m-2})\tau(x_{m+2})\tau^2(x_{m-1})+\tau^2(x_{m+3})\tau^3(x_{m-1}) \\ -\tau^2(x_{m-3})\tau^3(x_{m+1})-\tau(x_{m-3})\tau(x_{m+2})\tau(x_{m-2})\tau^2(x_{m+1}) \\ -\tau(x_{m-3})\tau^2(x_{m+2})\tau(x_{m-1})\tau(x_{m+1})-\tau(x_{m-3})\tau^3(x_{m+2})\tau(x_m) \\ -\tau(x_{m+3})\tau^2(x_{m-2})\tau^2(x_{m+1}) \\ -\tau(x_{m+3})\tau(x_{m-2})\tau(x_{m+2})\tau(x_{m-1})\tau(x_{m+1}) & ,x_m\le x<x_{m+1}\\ -\tau(x_{m+3})\tau(x_{m-2})\tau^2(x_{m+2})\tau(x_m)-\tau^2(x_{m+3})\tau^2(x_{m-1})\tau(x_{m+1})- \\ \tau^2(x_{m+3})\tau(x_{m-1})\tau(x_{m+2})\tau(x_m)-\tau^3(x_{m+3})\tau^2(x_m) \\ \tau(x_{m-3})\tau^4(x_{m+2})+\tau(x_{m+3})\tau(x_{m-2})\tau^3(x_{m+2}) \\ +\tau^2(x_{m+3})\tau(x_{m-1})\tau^2(x_{m+2})+\tau^3(x_{m+3})\tau(x_m)\tau(x_{m+2}) & ,x_{m+1}\le x<x_{m+2}\\ +\tau^4(x_{m+3})\tau(x_{m+1}) \\ -\tau^5(x_{m+3}) & ,x_{m+2}\le x<x_{m+3}\\ 0 & otherwise\end{cases}\tag{6}$$

where

$$\begin{aligned}\tau(x_m)&=\sin\left(\frac{x-x_m}{2}\right),\\ \theta&=\sin\left(\frac{h}{2}\right)\sin(h)\sin\left(\frac{3h}{2}\right)\sin(2h)\sin\left(\frac{5h}{2}\right),\\ m&=0(1)N.\end{aligned}$$

Let $U(x,t)$ and $V(x,t)$be approximate solution to $u(x,t)$ and $v(x,t)$ respectively, defined as

$$U(x,t)=\sum_{m=-2}^{N+2}\delta_m(t)T_m(x),V(x,t)=\sum_{m=-2}^{N+2}\phi_m(t)T_m(x)$$

where δ_m and ϕ_m are time dependent parameters that are by applying collocation procedure at the grid points $x_m, m=0,1,\dots,N$. Quintic trigonometric B-splines and its first four derivatives are continuous on element $[x_{m-3},x_{m+3}]$. The functional and derivative values of $U(x,t)$ (and $V(x,t)$) at a grid x_m can be obtained in terms of time dependent parameters δ (and ϕ) as

$$\begin{aligned}U_m&=U(x_m)=a_1\delta_{m-2}+a_2\delta_{m-1}+a_3\delta_m+a_2\delta_{m+1}+a_1\delta_{m+2},\\ U'_m&=U'(x_m)=b_1\delta_{m-2}+b_2\delta_{m-1}-b_2\delta_{m+1}-b_1\delta_{m+2},\\ U''_m&=U''(x_m)=c_1\delta_{m-2}+c_2\delta_{m-1}+c_3\delta_m+c_{2_{m+1}}+c_1\delta_{m+2},\\ U'''_m&=U'''(x_m)=d_1\delta_{m-2}+d_2\delta_{m-1}-d_2\delta_{m+1}-d_1\delta_{m+2}\\ U''''_m&=U''''(x_m)=e_1\delta_{m-2}+e_2\delta_{m-1}+e_3\delta_m+e_2\delta_{m+1}+e_1\delta_{m+2}.\end{aligned}\tag{7}$$

where

$$a_1=\sin^5(\tfrac{h}{2})/\theta$$
$$a_2=2\sin^5(\tfrac{h}{2})\cos(\tfrac{h}{2})\left(16\cos^2(\tfrac{h}{2})-3\right)/\theta$$
$$a_3=2\left(1+48\cos^4(\tfrac{h}{2})-16\cos^2(\tfrac{h}{2})\right)\sin^5(\tfrac{h}{2})/\theta$$
$$b_1=(-5/2)\sin^4(\tfrac{h}{2})\cos(\tfrac{h}{2})/\theta$$

$$b_2 = -5\sin^4(\tfrac{h}{2})\cos^2(\tfrac{h}{2})\left(8\cos^2(\tfrac{h}{2}) - 3\right)/\theta$$
$$c_1 = (5/4)\sin^3(\tfrac{h}{2})\left(5\cos^2(\tfrac{h}{2}) - 1\right)/\theta$$
$$c_2 = (5/2)\sin^3(\tfrac{h}{2})\cos(\tfrac{h}{2})\left(-15\cos^2(\tfrac{h}{2}) + 3 + 16\cos^4(\tfrac{h}{2})\right)/\theta$$
$$c_3 = (-5/2)\sin^3(\tfrac{h}{2})\left(16\cos^6(\tfrac{h}{2}) - 5\cos^2(\tfrac{h}{2}) + 1\right)/\theta$$
$$d_1 = (-5/8)\sin^2(\tfrac{h}{2})\cos(\tfrac{h}{2})\left(25\cos^2(\tfrac{h}{2}) - 13\right)/\theta$$
$$d_2 = (-5/4)\sin^2(\tfrac{h}{2})\cos^2(\tfrac{h}{2})\left(8\cos^4(\tfrac{h}{2}) - 35\cos^2(\tfrac{h}{2}) + 15\right)/\theta$$
$$e_1 = (5/16)\left(125\cos^4(\tfrac{h}{2}) - 114\cos^2(\tfrac{h}{2}) + 13\right)\sin(\tfrac{h}{2})/\theta$$
$$e_2 = (-5/8)\sin(\tfrac{h}{2})\cos(\tfrac{h}{2})\left(176\cos^6(\tfrac{h}{2}) - 137\cos^4(\tfrac{h}{2}) - 6\cos^2(\tfrac{h}{2}) + 15\right)/\theta$$
$$e_3 = (5/8)\left(92\cos^6(\tfrac{h}{2} - 17\cos^4(\tfrac{h}{2}) + 62\cos^2(\tfrac{h}{2}) - 13\right)\left(-1 + 4\cos^2(\tfrac{h}{2})\right)\sin(\tfrac{h}{2})/\theta$$

Applying of the Crank-Nicolson and the classical forward difference leads to

$$\begin{aligned}
&\frac{U^{n+1}-U^n}{\Delta t} + \frac{U_{xxx}^{n+1}+U_{xxx}^n}{2} + 3\alpha\frac{(U^2U_x)^{n+1}+(U^2U_x)^n}{2} + \alpha\frac{(V^2U_x)^{n+1}+(V^2U_x)^n}{2} + 2\alpha\frac{(UVV_x)^{n+1}+(UVV_x)^n}{2} = 0\\
&\frac{V^{n+1}-V^n}{\Delta t} + \frac{V_{xxx}^{n+1}+V_{xxx}^n}{2} + 2\alpha\frac{(UVU_x)^{n+1}+(UVU_x)^n}{2} + 3\alpha\frac{(V^2V_x)^{n+1}+(V^2V_x)^n}{2} + \alpha\frac{(U^2V_x)^{n+1}+(U^2V_x)^n}{2} = 0
\end{aligned} \tag{8}$$

where $U^{n+1} = U(x, t_n + \Delta t)$, $V^{n+1} = V(x, t_n + \Delta t)$. The nonlinear terms $(U^2U_x)^{n+1}$, $(V^2U_x)^{n+1}$, $(UVV_x)_x^{n+1}$, $(UVU_x)_x^{n+1}$, $(V^2V_x)^{n+1}$ and $(U^2V_x)^{n+1}$ in Eq. (8) are linearized by using the following forms [21]:

$$\begin{aligned}
(U^2U_x)^{n+1} &= 2U^{n+1}U^nU_x^n + (U^n)^2U_x^{n+1} - 2(U^n)^2U_x^n\\
(V^2U_x)^{n+1} &= 2V^{n+1}V^nU_x^n + (V^n)^2U_x^{n+1} - 2(V^n)^2U_x^n\\
(UVV_x)^{n+1} &= U^{n+1}V^nV_x^n + U^nV^{n+1}V_x^n + U^nV^nV_x^{n+1} - 2U^nV^nV_x^n\\
(UVU_x)^{n+1} &= U^{n+1}V^nU_x^n + U^nV^{n+1}U_x^n + U^nV^nU_x^{n+1} - 2U^nV^nU_x^n\\
(V^2V_x)^{n+1} &= 2V^{n+1}V^nV_x^n + (V^n)^2V_x^{n+1} - 2(V^n)^2V_x^n\\
(U^2V_x)^{n+1} &= 2U^{n+1}U^nV_x^n + (U^n)^2V_x^{n+1} - 2(U^n)^2V_x^n
\end{aligned}$$

Substitution the approximate solution (7) into (8) and evaluating the resulting equations at the knots yields the system of the fully-discretized equations

$$\begin{aligned}
&\mu_1\delta_{m-2}^{n+1} + \mu_2\phi_{m-2}^{n+1} + \mu_3\delta_{m-1}^{n+1} + \mu_4\phi_{m-1}^{n+1} + \mu_5\delta_m^{n+1}\\
&+\mu_6\phi_m^{n+1} + \mu_7\delta_{m+1}^{n+1} + \mu_8\phi_{m+1}^{n+1} + \mu_9\delta_{m+2}^{n+1} + \mu_{10}\phi_{m+2}^{n+1}\\
&= \mu_{11}\delta_{m-2}^n + \mu_{12}\phi_{m-2}^n + \mu_{13}\delta_{m-1}^n + \mu_{14}\phi_{m-1}^n + \mu_{15}\delta_m^n\\
&+\mu_{16}\phi_m^n + \mu_{17}\delta_{m+1}^n + \mu_{14}\phi_{m+1}^n + \mu_{18}\delta_{m+2}^n + \mu_{17}\phi_{m+2}^n
\end{aligned} \tag{9}$$

$$\begin{aligned}
&\mu_2\delta_{m-2}^{n+1} + \eta_1\phi_{m-2}^{n+1} + \mu_4\delta_{m-1}^{n+1} + \eta_2\phi_{m-1}^{n+1} + \mu_6\delta_m^{n+1}\\
&+\eta_3\phi_m^{n+1} + \mu_8\delta_{m+1}^{n+1} + \eta_4\phi_{m+1}^{n+1} + \mu_{10}\delta_{m+2}^{n+1} + \eta_5\phi_{m+2}^{n+1}\\
&= \eta_6\delta_{m-2}^n + \eta_7\phi_{m-2}^n + \eta_8\delta_{m-1}^n + \eta_9\phi_{m-1}^n + \eta_{10}\delta_m^n\\
&+\eta_{11}\phi_m^n + \eta_8\delta_{m+1}^n + \eta_{12}\phi_{m+1}^n + \eta_6\delta_{m+2}^n + \eta_{13}\phi_{m+2}^n
\end{aligned} \tag{10}$$

where

$$\mu_1 = \left(\frac{2}{\Delta t} + 6\alpha PQ + 2\alpha RS\right)a_1 + \alpha(3P^2 + R^2)b_1 + d_1$$
$$\mu_2 = 2\alpha(RQ + PS)a_1 + 2\alpha PRb_1$$
$$\mu_3 = \left(\frac{2}{\Delta t} + 6\alpha PQ + 2\alpha RS\right)a_2 + \alpha(3P^2 + R^2)b_2 + d_2$$
$$\mu_4 = 2\alpha(RQ + PS)a_2 + 2\alpha PRb_2$$
$$\mu_5 = \left(\frac{2}{\Delta t} + 6\alpha PQ + 2\alpha RS\right)a_3$$
$$\mu_6 = 2\alpha(RQ + PS)a_3$$
$$\mu_7 = \left(\frac{2}{\Delta t} + 6\alpha PQ + 2\alpha RS\right)a_2 - \alpha(3P^2 + R^2)b_2 - d_2$$
$$\mu_8 = 2\alpha(RQ + PS)a_2 - 2\alpha PRb_2$$
$$\mu_9 = \left(\frac{2}{\Delta t} + 6\alpha PQ + 2\alpha RS\right)a_1 - \alpha(3P^2 + R^2)b_1 - d_1$$
$$\mu_{10} = 2\alpha(RQ + PS)a_1 - 2\alpha PRb_1$$
$$\mu_{11} = \left(\frac{2}{\Delta t} + 3\alpha PQ + 2\alpha RS\right)a_1 - d_1$$
$$\mu_{12} = (\alpha RQ)a_1$$
$$\mu_{13} = \left(\frac{2}{\Delta t} + 3\alpha PQ + 2\alpha RS\right)a_2 - d_2$$
$$\mu_{14} = (\alpha RQ)a_2$$
$$\mu_{15} = \left(\frac{2}{\Delta t} + 3\alpha PQ + 2\alpha RS\right)a_3$$
$$\mu_{16} = (\alpha RQ)a_3$$
$$\mu_{17} = \left(\frac{2}{\Delta t} + 3\alpha PQ + 2\alpha RS\right)a_2 + d_2$$
$$\mu_{18} = \left(\frac{2}{\Delta t} + 3\alpha PQ + 2\alpha RS\right)a_1 + d_1$$

$$\eta_1 = \left(\frac{2}{\Delta t} + 6\alpha RS + 2\alpha PQ\right)a_1 + \alpha(3R^2 + P^2)b_1 + d_1$$
$$\eta_2 = \left(\frac{2}{\Delta t} + 6\alpha RS + 2\alpha PQ\right)a_2 + \alpha(3R^2 + P^2)b_2 + d_2$$
$$\eta_3 = \left(\frac{2}{\Delta t} + 6\alpha RS + 2\alpha PQ\right)a_3$$
$$\eta_4 = \left(\frac{2}{\Delta t} + 6\alpha RS + 2\alpha PQ\right)a_2 - \alpha(3R^2 + P^2)b_2 - d_2$$
$$\eta_5 = \left(\frac{2}{\Delta t} + 6\alpha RS + 2\alpha PQ\right)a_1 - \alpha(3R^2 + P^2)b_1 - d_1$$
$$\eta_6 = (\alpha PS)a_1$$
$$\eta_7 = \left(\frac{2}{\Delta t} + 2\alpha PQ + 3\alpha RS\right)a_1 - d_1$$
$$\eta_8 = (\alpha PS)a_2$$
$$\eta_9 = \left(\frac{2}{\Delta t} + 2\alpha PQ + 3\alpha RS\right)a_2 - d_2$$
$$\eta_{10} = (\alpha PS)a_3$$
$$\eta_{11} = \left(\frac{2}{\Delta t} + 2\alpha PQ + 3\alpha RS\right)a_3$$
$$\eta_{12} = \left(\frac{2}{\Delta t} + 2\alpha PQ + 3\alpha RS\right)a_2 + d_2$$
$$\eta_{13} = \left(\frac{2}{\Delta t} + 2\alpha PQ + 3\alpha RS\right)a_1 + d_1$$

$$P = a_1\delta_{m-2}^n + a_2\delta_{m-1}^n + a_3\delta_m^n + a_2\delta_{m+1}^n + a_1\delta_{m+2}^n$$
$$Q = b_1\delta_{m-2}^n + b_2\delta_{m-1}^n - b_2\delta_{m+1}^n - b_1\delta_{m+2}^n$$
$$R = a_1\phi_{m-2}^n + a_2\phi_{m-1}^n + a_3\phi_m^n + a_2\phi_{m+1}^n + a_1\phi_{m+2}^n$$
$$S = b_1\phi_{m-2}^n + b_2\phi_{m-1}^n - b_2\phi_{m+1}^n - b_1\phi_{m+2}^n$$

To have a solvable system, eight boundary conditions $U(a,t)=0$, $U_x(a,t)=0$, $U(b,t)=0, U_x(b,t)=0$, $V(a,t)=0$, $V_x(a,t)=0$, $V(b,t)=0, V_x(b,t)=0$ are used to have additional eight equations, so that system of dimension $(2N+2)\times(2N+10)$ is solved to have the $(2N+10)$ unknown parameters

$$\mathbf{x}^{n+1}=(\delta_{-2}^{n+1},\phi_{-2}^{n+1},\delta_{-1}^{n+1},\phi_{-1}^{n+1},\dots,\delta_{n+1}^{n+1},\phi_{n+1}^{n+1},\delta_{n+2}^{n+1},\phi_{n+2}^{n+1})$$

This system is solved with Matlab packet program using Gauss elimination.

Time evolution of parameters δ_m^{n+1} (and ϕ_m^{n+1}) are computed once the initial parameters δ_m^0 (and ϕ_m^0) are obtained with help of the boundary and initial conditions below:

$$\begin{aligned}
&U(a,0)=a_1\delta_{-2}^0+a_2\delta_{-1}^0+a_3\delta_0^0+a_2\delta_1^0+a_1\delta_2^0=0,\\
&U_x(a,0)=b_1\delta_{-2}^0+b_2\delta_{-1}^0-b_2\delta_1^0-b_1\delta_2^0=0,\\
&U(x,0)=a_1\delta_{m-2}^0+a_2\delta_{m-1}^0+a_3\delta_m^0+a_2\delta_{m+1}^0+a_1\delta_{m+2}^0=U(x_m,0), m=1(1)N-1\\
&U(b,0)=a_1\delta_{N-2}^0+a_2\delta_{N-1}^0+a_3\delta_N^0+a_2\delta_{N+1}^0+a_1\delta_{N+2}^0=0,\\
&U_x(b,0)=b_1\delta_{N-2}^0+b_2\delta_{N-1}^0-b_2\delta_{N+1}^0-b_1\delta_{N+2}^0=0.
\end{aligned}$$

4. NUMERICAL EXAMPLES

The maximum error norm measuring the error between the numerical and the analytical solutions, if exist, defined as

$$L_\infty=|w-W|_\infty=\max_m|w_m^n-W_m^n|$$

The conservation laws can also be good indicators of the validity of the numerical methods, especially when the analytical solutions do not exist. The lowest three conservation laws are defined as

$$I_1=\int_{-\infty}^{\infty} w dx$$

$$I_2=\int_{-\infty}^{\infty} |w|^2 dx$$

$$I_3=\int_{-\infty}^{\infty} \frac{\alpha}{2}(|w|^4-|w_x|^2)dx$$

The conserved quantities are taken from the paper [22]. The absolute relative changes $C(I_1^t)$, $C(I_2^t)$ and $C(I_3^t)$ of the conservation laws I_1, I_2 and I_3 are

$$C(I_1^t)=\left|\frac{I_1^t-I_1^0}{I_1^0}\right|$$

$$C(I_2^t)=\left|\frac{I_2^t-I_2^0}{I_2^0}\right|$$

$$C(I_3^t)=\left|\frac{I_3^t-I_3^0}{I_3^0}\right|$$

where I_1^0, I_2^0 and I_3^0 are initial quantities, I_1^t, I_2^t and I_3^t are the numerically computed values of the conserved quantities at the time t.

4.1. Motion of Single Solitary Wave

The CMKdV equation has complex valued exact solutions [2]

$$w(x,t) = \sqrt{\frac{2c}{\alpha}}\operatorname{sech}\left[\sqrt{c}(x - x_0 - ct)\right]\exp(i\theta_0) \tag{11}$$

describing propagation of an initial pulse of height $\sqrt{\frac{2c}{\alpha}}$ with constant velocity c moving along space axis, θ_0 denotes the angle of polarization. The parameters are chosen as $c = 1, \alpha = 2, x_0 = -15, \theta_0 = \pi/4$ for convenience. This form of the equation is a good describer for non-linear evolution of plasma waves.

The boundary conditions are adapted to the numerical method at both end of the finite interval $[-20,60]$. The suggested algorithm is run for the time step $\Delta t = 0.001$ and five varying spatial steps to make comprasion with the results of the quintic B-spline collocation method [4] given at the $t = 3$ in Table 1. Generally, the error is reduced by one decimal digits by use of the trigonometric B-spline collocation method for getting the solution of CMKdV.

Table 1. Comparison of the $L_\infty \times 1000$ for the single soliton for $\Delta t = 0.001$ at $t = 3$ various *N*.

N	Trigonometric spline	Polynomial spline [4]
300	0.09013	0.41519
400	0.02468	0.13715
600	0.00444	0.02589
800	0.00115	0.00780
1000	0.00044	0.00293

A three dimensional simulation of the propagation is depicted in Figure 1a and the maximum error distributions of the solution obtained by present method at the simulation terminating time is depicted in Figure 1b. The designed routines are run to the terminating time $\boldsymbol{t = 3}$ with the discretization parameters $\boldsymbol{N = 1000}$ and $\boldsymbol{\Delta t = 0.001}$ in the finite problem interval $[\boldsymbol{-20, 60}]$. Maximum error occurs around the peak of solitary wave seeing in Figure 1b.

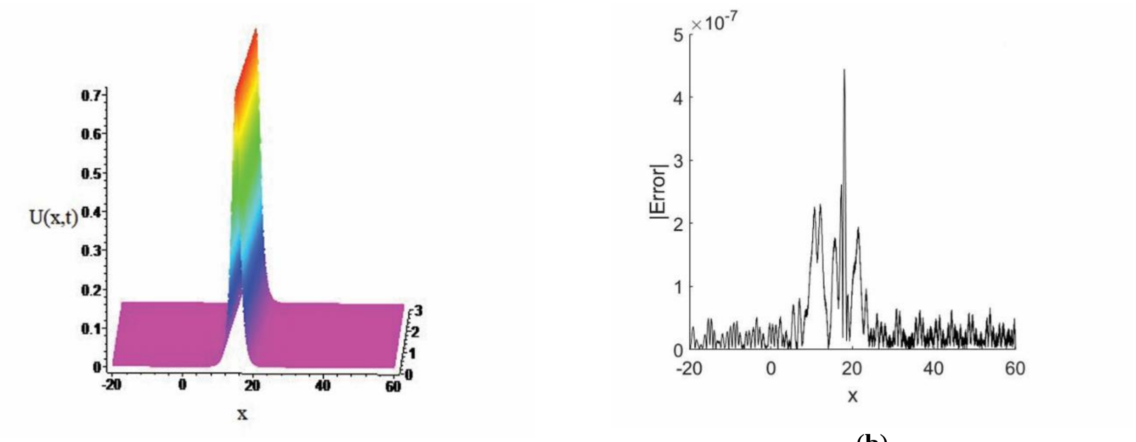

(a) (b)

Figure 1. Propagation of the initial pulse and the maximum absolute error at t=3.

The initial exact values of the conservation laws are computed using the initial conditions over $[-20,60]$ as as

$$I_1^0 = 3.14159265$$
$$I_2^0 = 2.00000000$$
$$I_3^0 = 0.66666677$$

The conservation laws are calculated using the numerical solution at the grid points for the parameters $\Delta t = 0.001$ and the spatial steps at the $t = 3$. Conservation quantities remain constants and the relative error becomes smaller when the number of grid points are increases seen in Table 2.

Table 2. Conservative laws and their relative changes for $\Delta t = 0.001$ at $t = 3$ various N.

N	I_1^0	I_2^0	I_3^0	$C(I_1^3)$	$C(I_2^3)$	$C(I_3^3)$
300	3.14159265	2.00000000	0.66666738	0.00023078	0.0000000104	0.0000003766
400	3.14159265	2.00000000	0.66666678	0.00003031	0.0000000000	0.0000000134
600	3.14159265	2.00000000	0.66666668	0.00000385	0.0000000002	0.0000000008
800	3.14159265	2.00000000	0.66666667	0.00000093	0.0000000002	0.0000000005
1000	3.14159265	2.00000000	0.66666667	0.00000038	0.0000000002	0.0000000005

4.2. Interaction of Two Solitary Waves

The interaction of two solitary waves is studied by using the inital condititon [5]:

$$w(x,0) = \sqrt{\frac{2c_1}{\alpha}}\,\mathrm{sec}h[\sqrt{c_1}(x - x_1)]\exp(i\theta_1) + \sqrt{\frac{2c_2}{\alpha}}\,\mathrm{sec}h[\sqrt{c_2}(x - x_2)]\exp(i\theta_2)$$

This initial condition represents two solitary waves, one positioned around x_1, the other one around x_2 initially. The artifical problem interval is chosen as $[0,100]$. The remaining parameters are chosen as $c_1 = 2, c_2 = 0.5, \theta_1 = 0,\ \theta_2 = \frac{\pi}{2}, x_1 = 25$ and $x_2 = 50$. The program is run until time $t = 25$ with the discretization parameters $N = 500$ and $\Delta t = 0.001$ over the interval $[0,100]$. The propogation of two solitary waves with different amplitudes travelling in the x-axis. After the interaction, they conserve the original shapes rights is observed to pass through each other and keep their magnitudes after the interaction in Figures 2. When the time reaches $t = 10$, it is observed that the interaction has started, Figure 2b. The height of the higher solitary is measured as 1.4145 and its peak is positioned at $x = 45$. The height of the lower one increases to 0.7071 and the position of its peak is determined as $x = 55$. The height of the higher wave reaches 1.1790 as the height of the lower one 0.7898 at the time $t = 15$, Figure 2c. The peaks of both the higher and the lower solitaries are positioned at $x = 54.8$ and $x = 57.4$, respectively. When the time reaches $t = 16$, the solitaries begin to separate, Figure 2d. In Figure 2e, the height of the higher one increases to 1.4408 and it is positioned at $x = 66.6$. The peak of the lower one is positioned at $x = 56.8$ and the height of it decreased to 0.6372. At the end of the simulation, we observe both solitaries are separated completely and return to their original shapes and heights, Figure 2f. The heights of both solitaries are determined as 0.6028 and 1.4411 as the peaks reach $x = 58.6$ and 77.2 as keeping to propagate on their own ways.

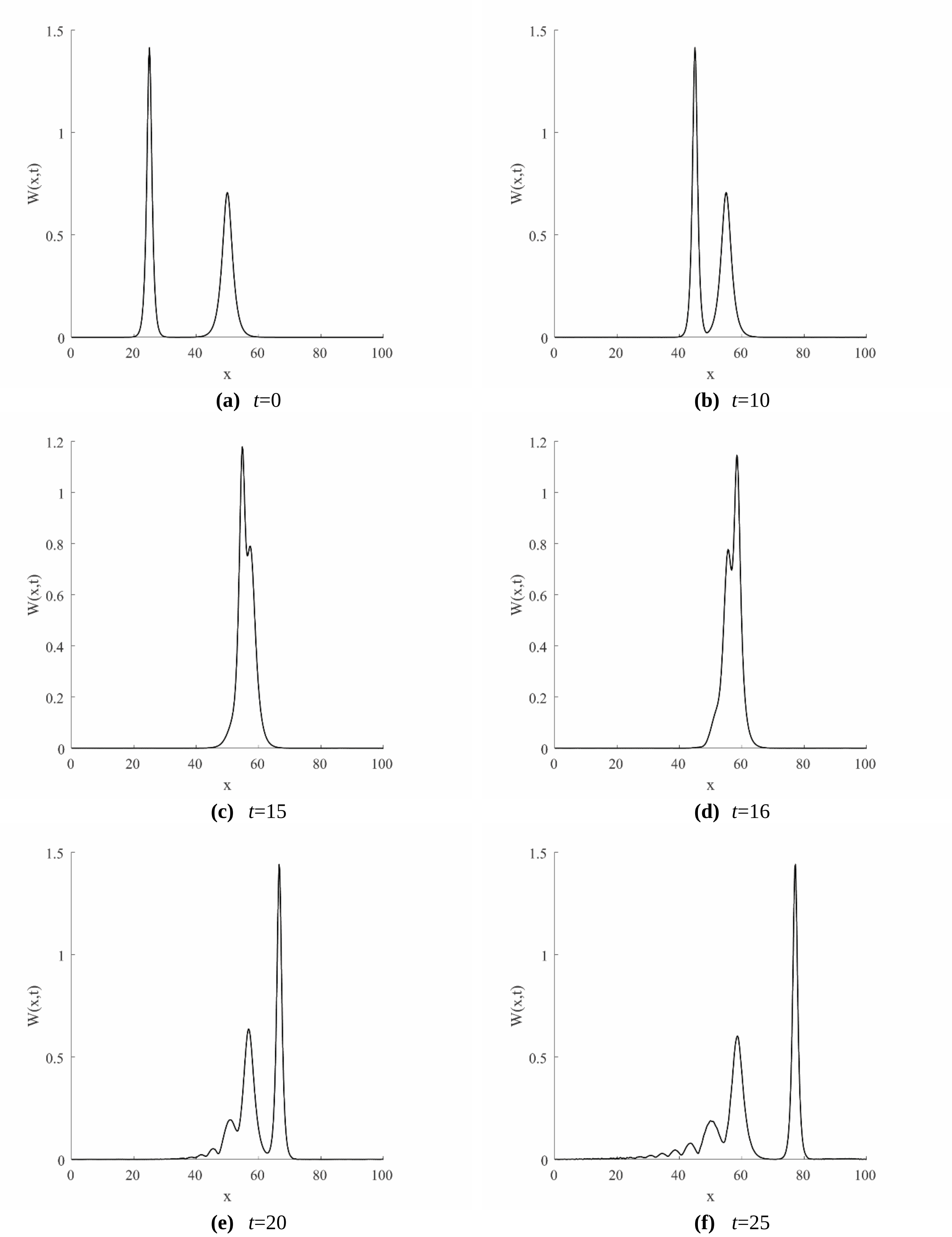

Figure 2. Interaction of two solitary waves.

4.3. Interaction of Three Solitary Waves

The collusion of three solitary waves is simulated by studying with the initial data [5],

$$w(x,0) = \sum_{j=1}^{3} \sqrt{\frac{2c_j}{\alpha}}\operatorname{sech}\left[\sqrt{c_j}\left(x - x_j\right)\right]\exp(i\theta_j)$$

The three solitary waves are well seperated and their peaks are located at x_1, x_2 and x_3. All moves to the right as time proceeds. The algorithm is run in the artificial interval $[0,100]$ with the parameters $x_1 = 10, x_2 = 30, x_3 = 50$ up to time $t = 80$. We assume that $c_1 = 1, c_2 = 0.5, c_3 = 0.3, \theta_1 = 0, \theta_2 = 0$ and $\theta_3 = 0$.

This initial condition gives three positive bell shaped solitaries of heights 1.0000, 0.7071 and 0.5477 positioned $x = 10$, $x = 20$ and $x = 30$ respectively in Figure 3a. All solitaries propagate in the same directions along the horizontal axis as time goes. Interaction of three solitary waves are exhibited in Figures 3.

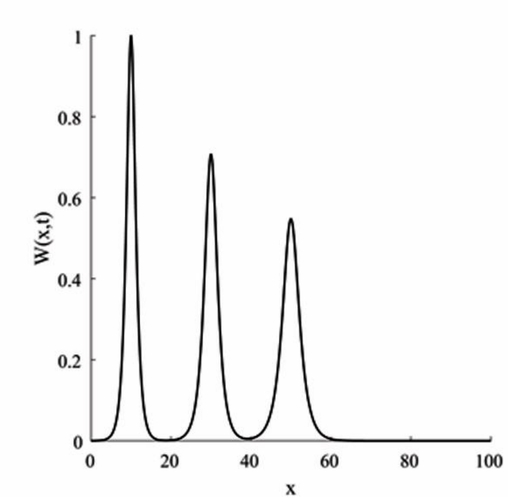

(a) *t*=0

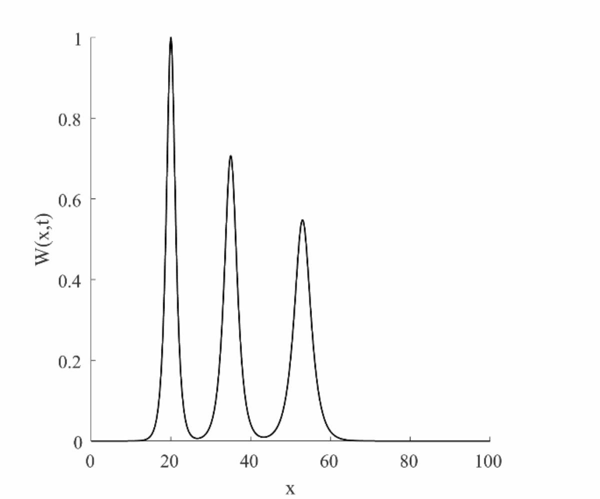

(b) *t*=10

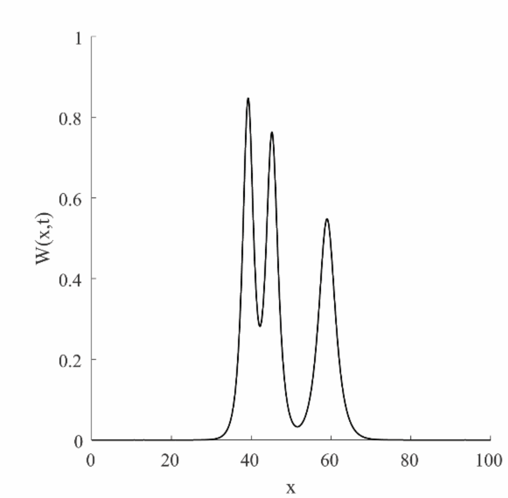

(c) *t*=30

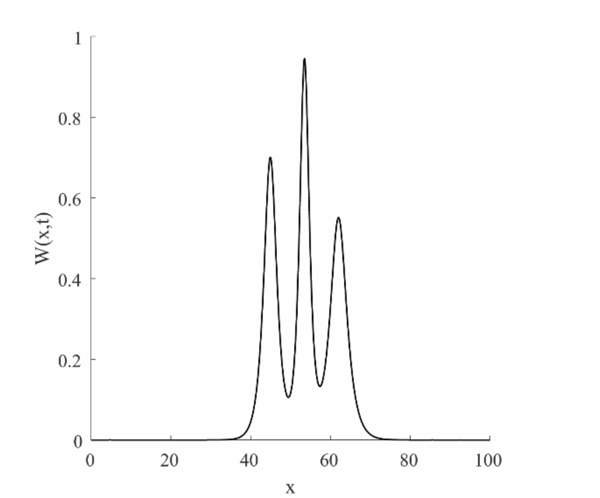

(d) *t*=40

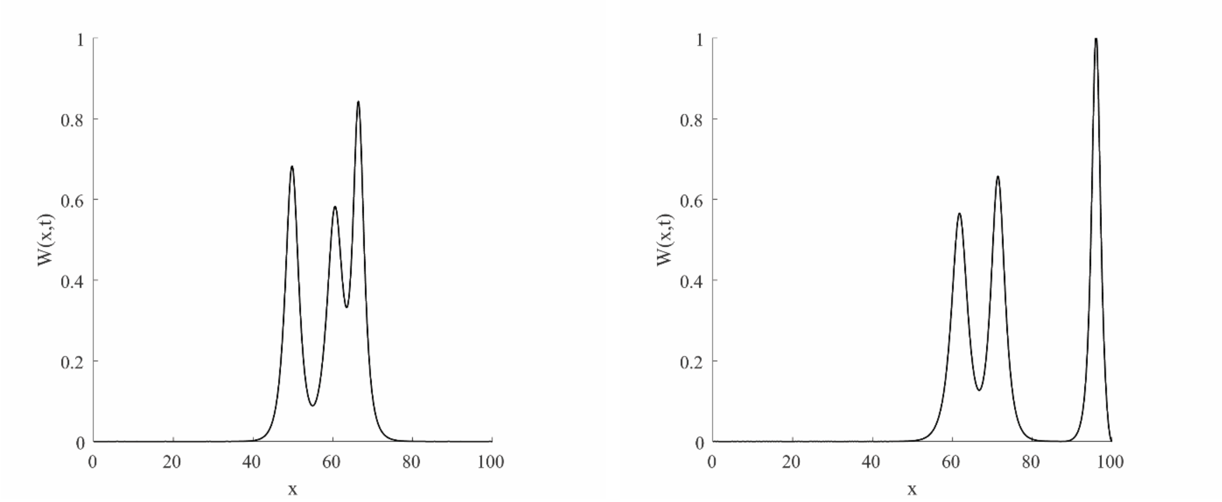

(e) t=50 **(f)** t=80

Figure 3. Interaction of three solitary waves

The conserved laws are given in Table 3 for varios t and fixed $\Delta t = 0.001, N = 1000$. The values are computed as $I_1^0 = 9.42468708$, $I_2^0 = 4.51000556$ and $I_3^0 = 1.01209702$ initially. According the Table 3, these are almost constant during the interaction simulation.

Table 3. Conservative laws and their relative changes for $\Delta t = 0.001$ and $N = 1000$ various t

t	I_1^t	I_2^t	I_3^t	$C(I_1^t)$	$C(I_2^t)$	$C(I_3^t)$
0	9.42468708	4.51000556	1.01209702			
10	9.42523161	4.51000556	1.01209687	0.00005778	0.000000000	0.000000015
30	9.42541556	4.51000546	1.01209781	0.00007729	0.000000022	0.000000078
40	9.42558213	4.51000553	1.01209714	0.00009497	0.000000005	0.000000012
50	9.42574272	4.51000549	1.01209755	0.00011201	0.000000015	0.000000052
80	9.31891836	4.51001022	1.00628948	0.01122252	0.000001034	0.000573813

5. CONCLUSION

Based on quintic trigonometric B-spline functions, a collocation approach has been implemented to some initial boundary value problems for the CMKdV equation. To be able obtain numerical solutions, firstly CMKdV equation was converted to a system of ordinary differential equations. The Crank–Nicolson scheme was used to discretize both equation in time variable. Quintic trigonometric B-spline functions were used for the space integration. Resultant ordinary differential equation system was solved via Gauss elimination using Matlab programme language. The validity of the method was checked by computing maximum error in the first problem. Then, absolute relative changes of the lowest three conserved quantities were computed for first and third test problems. The conserved quantities were preserved during the simulations. The preservation of conservation quantities shows the efficiency of the algorithm. As a conclusion, quintic trigonometric B-spline collocation method gives numerical solutions of the CMKdV equation with high accuracy.

ACKNOWLEDGMENTS

This study was partially presented at International Conference on Mathematics and Engineering, Istanbul, Turkey, 2017.

REFERENCES

[1] Wazwaz AM. The tanh and the sine–cosine methods for the complex modified KdV and the generalized KdV equations. Comput. Math Appl 2005; 49: 1101–1112.

[2] Muslu GM, Erbay HA. A spliet step fourier Method for the Complex Modified Korteweg De Vries Equation. Computers and Mathematics with Aplplications, 2003; 45: 503–514.

[3] Taha TR, Numerical simulations of the complex modified Korteweg-de Vries equation. Mathematics and Computers in Simulation 1994; 37: 461-467.

[4] Irk D. B-spline Finite Element Solutions of the Some Partial Differential Equation Systems, Department of Mathematics. Doctoral Dissertation, (2007).

[5] Ismail MS. Numerical solution of complex modified Korteweg-de Vries equation by collocation method. Communications in Nonlinear Science and Numerical Simulation. 2009;14: 749–759.

[6] Ismail MS. Numerical solution of complex modified Korteweg–de Vries equation by Petrov–Galerkin method. Applied Mathematics and Computation. 2008; 202: 520–531.

[7] Korkmaz A, Dag, I. Solitary wave simulations of Complex Modified Korteweg–de Vries Equation using differential quadrature method. Computer Physics Communications. 2009; 180: 1516–1523.

[8] Korkmaz A, Dag I. Numerical Simulations of Complex Modified KdV Equation using Polynomial Differential Quadrature Method. J of Mathematics and Statistics. 2011; 10: 1-13.

[9] Korkmaz A, Dag I. Quartic and quintic B-spline methods for advection–diffusion equation. Applied Mathematics and Computation. 2016; 274: 208-219.

[10] Ersoy O, Korkmaz A, Dag I. Exponential B-Splines for Numerical Solutions to Some Boussinesq Systems for Water Waves. Mediterranean Journal of Mathematics. 2016; 13(6): 4975–4994.

[11] Korkmaz A, Ersoy O, Dag I. Motion of Patterns Modeled by the Gray-Scott Autocatalysis System in One Dimension. MATCH Communications in Mathematical and in Computer Chemistry. 2017; 77(2), 507-526.

[12] Uddin M, Haq S, Islam S. Numerical solution of complex modified Korteweg de Vries equation by mesh-free collocation method. Computers and Mathematics with Applications. 2009; 58: 566-578.

[13] Nikolis A. Numerical Solutions of Ordinary Differential Equations with Quadratic Trigonometric Splines. Applied Mathematics E-Notes. 1995; 4:142-149.

[14] Nikolis A, Seimenis I. Solving Dynamical Systems with Cubic Trigonometric Splines. Applied Mathematics E-notes. 2005; 5: 116-123.

[15] Abbas M, Majid AA, Ismail Md, Rashid A. The Application of Cubic Trigonometric B-spline to the Numerical Solution of the Hyperbolic Problems. Applied Mathematica and Computation. 2014; 239: 74-88.

[16] Abbas M, Majid AA, Ismail Md, Rashid A. Numerical Method Using Cubic Trigonometric B-spline Technique for non-classical Diffusion Problems. Abstract and applied analysis. (2014).

[17] Dag I, Irk D, Kacmaz O, Adar N. Trigonometric B-spline collocation algortihm for solving the RLW equation. Applied and Computational Mathematics. 2016; 15(1): 96-105.

[18] Hepson OE, Dag I. The Numerical Approach to the Fisher's Equation via Trigonometric Cubic B-spline Collocation Method. Communications on Nonlinear Analysis. 2017; 2: 91-100.

[19] Dag I, Ersoy O, Kacmaz O. The Trigonometric Cubic B-spline Algorithm for Burgers' Equation. International Journal of Nonlinear Science, 2017; 24(2): 120-128.

[20] Keskin P. Trigonometric B-spline solutions of the RLW equation. Department of Mathematics & Computer. Doctoral Dissertation. (2017).

[21] Rubin SG, Graves RA. Cubic spline approximation for problems in fluid mechanics. Nasa TR R-436 Washington DC (1975).

[22] Charles F. Karney F. Nonlinear evolution of lower hybrid waves. The Physics of Fluids. 1979; 22, 940.